Bose-Einstein condensate in a light-induced vector gauge potential using 1064-nm optical-dipole-trap lasers

Zhengkun Fu (付正坤), Pengjun Wang (王鹏军), Shijie Chai (柴世杰), Lianghui Huang (黄良辉), and Jing Zhang (张靖)*

State Key Laboratory of Quantum Optics and Quantum Optics Devices, Institute of Opto-Electronics, Shanxi University, Taiyuan 030006, P.R. China

(Received 3 June 2011; revised manuscript received 28 July 2011; published 7 October 2011)

Using two crossed 1064-nm optical-dipole-trap lasers to be the Raman beams, an effective vector gauge potential for Bose-Einstein condensed ^{87}Rb in the $F = 2$ hyperfine ground state is experimentally created. The moderate strength of the Raman coupling still can be achieved when the detuning from atomic resonance is larger than the excited-state fine structure, since rubidium has 15 nm energy-level spitting. The atoms at the far detuning of the Raman coupling are loaded adiabatically into the dressed states by ramping the homogeneous bias magnetic field with different paths and the dressed states with different energies are studied experimentally. The experimental scheme can be easily extended to produce the synthetic magnetic or electric field by means of a spatial or time dependence of the effective vector potential.

DOI: 10.1103/PhysRevA.84.043609 PACS number(s): 67.85.Hj, 03.75.Lm

Quantum degenerate gases in ultracold temperature offer us opportunities to efficiently simulate quantum condensed matter systems [1]. It is an important advantage for experiments that the physical parameters of atomic systems, including the number of the trapped atoms, the shape of the trapping potential, and the strength of the atom-atom interaction can be precisely controlled. A fascinating example of utilizing atomic systems is that the vector potential of the charged particles in a magnetic field can be simulated by the ultracold atomic gas if a gauge field is applied to it. In this case, the strongly correlated states of matter, such as the fractional quantum Hall effect exhibited by electrons in a magnetic field, can be easily studied. A well-known method is to rotate the gas [2,3] where the transformation to the rotating frame corresponds to giving the particles a fictitious charge, and applying an effective uniform magnetic field. Another approach is to induce gauge potentials through the laser-atom interactions [4,5]. There are already various theoretical proposals for generating artificial Abelian and non-Abelian gauge fields without [6–10] or with optical lattices [11–17], and some exotic properties are predicted [6–21]. The experiment on the generation of synthetic gauge fields has had made great progress recently in the NIST group [22–25]. In the Lin *et al*. experiment [22], the effective vector potential is generated by coupling a pair of 804.3 nm Raman laser beams into the magnetic sublevels of the $F = 1$ hyperfine level of the electronic ground state in a 1550 nm optically trapped Bose-Einstein condensate (BEC) of ^{87}Rb atoms. Successively, the synthetic magnetic [23] and electric fields [24] were also produced from a spatial variation and time dependence of the effective vector potential. Very recently, using the similar scheme BEC with spin-orbit coupling [25] has also been realized by the same group.

In this paper we report an experimental scheme of generating light-induce vector gauge potential, in which the two 1064-nm optical-dipole-trap lasers are also used as a pair of Raman lasers in ^{87}Rb BEC. At first an optically trapped BEC is created by the two crossed optical-dipole-trap lasers. Simultaneously, the two dipole-trap lasers with a frequency difference resonant with the energy difference between the magnetic sublevels, couple these two magnetic sublevels of the $F = 2$ hyperfine level of the electronic ground state. We adiabatically load the atoms at the far detuning of the Raman coupling into the dressed state by ramping the bias magnetic field to resonance. The different energy dressed states are loaded and studied. The collision decay of the high-energy dressed state is observed. The light-induced vector gauge potential by four-photon Raman process with $4\hbar k_R$ momentum is also observed. Our experimental setup can be easily extended to present the spatial or time dependent vector potential for producing synthetic magnetic or electric field.

The model with two-level system in Refs. [10,25] is employed in the experiment. We choose the two magnetic sublevels $|\uparrow\rangle = |F = 2, m_F = 2\rangle$ and $|\downarrow\rangle = |F = 2, m_F = 1\rangle$ of the $F = 2$ hyperfine level of the electronic ground state to be the two internal spin states, which are coupled by a pair of Raman beams with strength Ω. Two Raman beams have frequencies ω_R and $\omega_R + \nu_R$, and a bias field B along $\hat{x}$ produces a Zeeman shift $\hbar\omega_Z = g\mu_B B$. Since the momentum transfer induced by the Raman beams is along $\hat{x}$, the Hamiltonian is written as $H = H_R(k_x) + [\hbar^2(k_y^2 + k_z^2)/2m + V(\bar{r})]$, where $H_R(k_x)$ is the Hamiltonian for the Raman coupling, the Zeeman energies, and the motion along $\hat{x}$. $V(\bar{r})$ is the state-independent trapping potential arising from the scalar light trap of the Raman beams and m is the atomic mass. Under the rotating-wave approximation in the frame rotating at ν_R, the Hamiltonian $H_R(k_x)$ is written in the bare atomic state basis of $\{|\uparrow, k_x = p + k_R\rangle, |\downarrow, k_x = p - k_R\rangle\}$

$$H_R(k_x) = \hbar \begin{pmatrix} \frac{\hbar}{2m}(p + k_R)^2 - \delta/2 & \Omega/2 \\ \Omega/2 & \frac{\hbar}{2m}(p - k_R)^2 + \delta/2 \end{pmatrix}. \quad (1)$$

Here $\delta = \nu_R - \omega_Z$ is the detuning from Raman resonance, Ω is the resonant Raman Rabi frequency, p denotes quasi-momentum. $k_R = k_r \sin(\theta/2)$, $k_r = 2\pi/\lambda$ is the single-photon recoil momentum, λ is the wavelength of the Raman beam,

*Corresponding author: jzhang74@yahoo.com, jzhang74@sxu.edu.cn

and $\theta = 90^\circ$ is the intersecting angle of two Raman beams. $\hbar k_R$ and $E_R = (\hbar k_R)^2/2m = h \times 1.013$ kHz are the units of momentum and energy, respectively. $H_R(k_x)$ are diagonalized to get two energy eigenvalues $E_\pm(p) = \hbar[\hbar(p^2 + k_R^2)/2m \pm \sqrt{(4\hbar pk_R/2m - \delta)^2 + \Omega^2}/2]$, which give the effective dispersion relations of the dressed states. The two dressed eigenstates are expressed by

$$|\uparrow', p\rangle = c_1|\uparrow, k_x = p + k_R\rangle + c_2|\downarrow, k_x = p - k_R\rangle,$$
$$|\downarrow', p\rangle = c_3|\uparrow, k_x = p + k_R\rangle + c_4|\downarrow, k_x = p - k_R\rangle. \quad (2)$$

Here $c_1 = 1/\sqrt{a^2+1}$, $c_2 = a/\sqrt{a^2+1}$, and $a = -(4\hbar pk_R/2m - \delta - \sqrt{(4\hbar pk_R/2m - \delta)^2 + \Omega^2})/\Omega$. $c_3 = 1/\sqrt{b^2+1}$, $c_4 = b/\sqrt{b^2+1}$, and $b = -(4\hbar pk_R/2m - \delta + \sqrt{(4\hbar pk_R/2m - \delta)^2 + \Omega^2})/\Omega$. $|\uparrow', p\rangle$ is the high-energy dressed state for $E_+(p)$ and $|\downarrow', p\rangle$ is the low-energy dressed state for $E_-(p)$. Since the high and low energies $E_\pm$ of the dressed states depend on the experimental parameters Ω and δ, the positions of energy minima ($p_{\min}$) are thus experimentally tunable. For $\Omega < 4E_R$ and small δ, the lowest energy $E_-(p)$ consists of double wells in quasimomentum space. As $\Omega > 4E_R$, the double wells merge into a single well.

In our experiment, the optical-dipole trap is composed of two horizontal crossed beams at 90° along $\hat{y} \pm \hat{x}$ and overlapped at the focus, which also are used as two Raman beams (as shown in Fig. 1). The linear polarization of both beams is horizontal in the plane of x-y. Both beams are extracted from a 15 W laser (MOPA 15 NE, InnoLight Technology, Ltd.) operating at the wavelength of 1064 nm with the narrow linewidth single frequency. Two beams single-pass through two acousto-optic modulators (AOM) (3110-197, Crystal Technology, Inc.). The Raman beam 1 and 2 are frequency shifted −100 and −110.4 MHz by two signal generators (N9310A, Agilent), respectively. The frequency difference $\nu_R/2\pi = 10.4$ MHz of two signal generators are phase locked by a source locking cw microwave frequency counters (EIP 575B, Phase Matrix Inc.). Thus two laser beams are phase locked and frequency shifted 10.4 MHz relative to each other to avoid any spatial interference between the two beams, and at the same time provide the radio-frequency Raman coupling between two magnetic sublevels. Then two beams are coupled into two high power polarization maintaining single-mode fibers in order to increase stability of the beam pointing and obtain better beam-profile quality. Behind the fibers, one beam is focused to a waist size of $1/e^2$ radii of 38 μm by a achromatic lens of focus length $f = 300$ mm, and the other beam is focused to 49 μm by a $f = 400$ mm lens. For enhancing the intensity stability of the two beams, a small fraction of the light is sent into a photodiode and the regulator is used for comparing the intensity measured by the photodiode to a set voltage value from the computer. The nonzero error signal is compensated by adjusting the radio power in the AOM in front of the optical fiber.

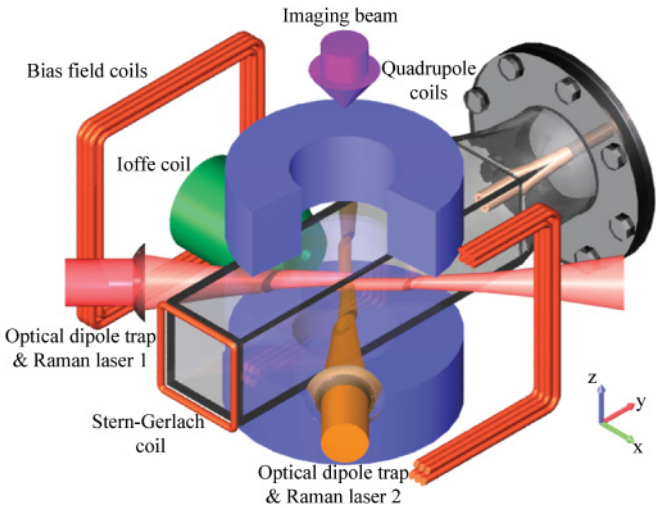

FIG. 1. (Color online) Schematic drawing of the experimental setup.

A homogeneous bias magnetic field provided by a pair of Helmholtz coils along $\hat{x}$ gives a linear Zeeman shift $\omega_Z/2\pi$ between two magnetic sublevels (as shown in Fig. 1). To control the magnetic field precisely and reduce the magnetic field noise, the power supply (Delta SM70-45D) has been operated in remote voltage programming mode, whose voltage is set by an analog output of the experiment control system. The current through the coils is controlled by the external regulator relying on a precision current transducer (Danfysik ultastable 867-60I). The output error signal from the regulator actively stabilize the current with the PID (proportional-integral-derivative) controller acting on the MOSFET (metal-oxide-semiconductor field-effect transistor). In order to reduce the current noise and decouple the control circuit from the main current, a conventional battery is used to power the circuit.

In our experiment, ^{87}Rb atoms are first precooled to 1.5 μK by radio-frequency evaporative cooling in a quadrupole-Ioffe configuration (QUIC) trap [26,27]. Subsequently, the atom sample is transferred back to the center of the glass cell [28] in favor of the optical access. After loading ^{87}Rb atoms in hyperfine state $|F = 2, m_F = 2\rangle$ into the dipole trap with the full powers (900 mW and 1.3 W) at a weak homogeneous bias magnetic field about 1 G, the forced evaporative cooling is performed by lowering the powers of two beams [29]. With the evaporation time of 1.2 s, the pure BEC with the atomic number of 2×10^5 is obtained at the powers of 169 (beam 1) and 320 mW (beam 2). In order to increase the Raman coupling strength, the powers of two dipole trap beams are increased to 207 (beam 1) and 480 mW (beam 2), respectively. The pure BEC is still maintained in the dipole trap with trap frequency of $2\pi \times 83$ Hz along $\hat{x}$ and $\hat{y}$. Now we first measure the resonant Raman Rabi frequency Ω by observing population oscillations driven by the variable Raman pulse length. The third dipole trap beam (beam 3) with frequency shifted −103 MHz counterpropagating with the Raman beam 2 is utilized in the measurement process. The BEC is loaded adiabatically into the crossed dipole trap composed of Raman beam 1 and dipole trap beam 3 by ramping the dipole trap beam 3 and decreasing the intensity of the Raman beam 2 to zero. Then the homogeneous bias magnetic field is ramped to the value with $\hbar\delta = -4E_R$, so the atoms are resonant for $|\uparrow', 0\rangle \rightarrow |\downarrow', -2k_R\rangle$ [the energy gap $E_+(p = -k_R) - E_-(p = -k_R) = \hbar\Omega$]. By the variable Raman pulse length of Raman beam 2, the observed oscillation period of 420 μs corresponds to the resonant Raman Rabi frequency $\hbar\Omega = 2.35E_R$.

We adiabatically load the BEC initially in $|\uparrow,0\rangle$ into the Raman-dressed states of the low E_- or high energy E_+, simply by ramping the homogeneous bias magnetic field with the different paths. Here, when the atoms are Raman resonant (at 10.4 MHz with $\delta = 0$) between $|\uparrow\rangle$ and $|\downarrow\rangle$, the detuning between $|\downarrow\rangle$ and $|F = 2, m_F = 0\rangle$ is about $-30E_R$, we may regard it as the two-level system. At last, the Raman dressed states may be characterized by the time-of-flight (TOF). When the Raman beams and the homogeneous bias magnetic field are turned off abruptly, the atoms are projected onto its individual spin and momentum components. The atoms then expand in a magnetic field gradient for 28 ms during TOF along $\hat{y}$, and the two spin states are separated spatially due to the Stern-Gerlach effect. Imaging the atoms after a 30 ms TOF gives the momentum and spin composition of the dressed state. Now we discuss three cases of loading the BEC into the Raman-dressed states by ramping the homogeneous bias magnetic field with three different paths.

Case 1. We prepare the BEC initially in $|\uparrow,0\rangle$ locating in the low energy branch E_- with the far positive detuning $\hbar\delta \gg E_R$ by setting the homogeneous bias magnetic field at the value of $B \ll B_0$, as shown in Figs. 2(a) and 2(b). Here B_0 corresponds to the $\delta = 0$. Then we ramp the homogeneous bias magnetic field slowly in a time 150 ms to the value with $\hbar\delta = 2E_R$ and hold on in a variable time t_h. Since $\Omega < 4E_R$ in the experiment, the low energy $E_-(p)$ presents the double wells in quasimomentum space. When $\hbar\delta = 2E_R$, the double wells become asymmetry and the low-energy well locates at $p_{\min} = -0.925k_R$. Thus the atoms are loaded to low-energy dressed state adiabatically and locate low-energy well of the double wells at $p_{\min} = -0.925k_R$. Figure 2(c) shows spin-resolved TOF images of adiabatically loaded the dressed state with the different holding times. These images demonstrate that the atoms are loaded to low-energy dressed state adiabatically at the low-energy well of the double wells, which are very stable with the long lifetime.

Case 2. The initial condition is the same as case 1. The difference is that the homogeneous bias magnetic field is ramped to the value with $\hbar\delta = -E_R$ $(B > B_0)$ as shown in Fig. 3(a). The low-energy well of the asymmetry double wells is changed into $p_{\min} = 0.889k_R$. The atoms still are loaded to low-energy dressed state adiabatically, however locate at high-energy well (no $p_{\min}$) of the double wells as shown Fig. 3(b). The dressed atoms locating at high-energy well of the double wells are unstable and will transit to the low-energy well. Images in Fig. 3(c) show this transition process. After holding time of 20 ms, the dressed atoms populate the low-energy well of the double wells.

Case 3. We prepare the BEC initially in $|\uparrow,0\rangle$ locating in the high energy branch E_+ with the far negative detuning $\hbar\delta \ll -E_R$ by setting the homogeneous bias magnetic field at the value of $B > B_0$, as shown in Figs. 4(a) and 4(b).

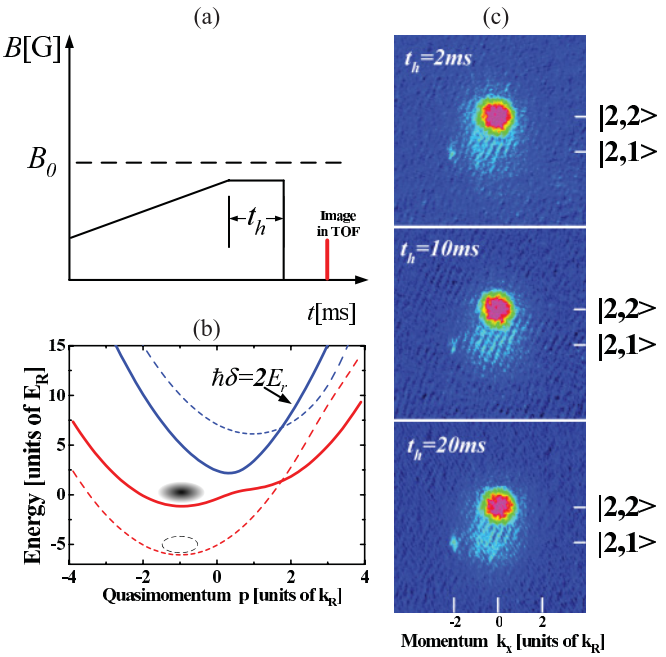

FIG. 2. (Color online) (a) The time sequence of the homogeneous bias magnetic field for loading the atoms into the low-energy Raman-dressed state. The horizontal dashed line indicates B_0, which corresponds to $\delta = 0$. (b) Energy-quasimomentum dispersion for $\hbar\delta = 2E_R$ (thick solid curves) and $\hbar\delta \gg E_R$ (thin dashed curves) at Raman coupling strength $\hbar\Omega = 2.35E_R$. The quasimomentum of BEC keeps in the low-energy dressed state with $p_{\min} < 0$ for $B < B_0$. (c) Images (1.17 mm by 1.17 mm) of the Raman-dressed state for $\hbar\delta = 2E_R$ with variable hold times t_h after a 30 ms TOF. The two spin and momentum components $|\uparrow, k_x = p_{\min} + k_R\rangle$ and $|\downarrow, k_x = p_{\min} - k_R\rangle$ are separated along $\hat{y}$ (a Stern-Gerlach field is applied along $\hat{y}$ before the image).

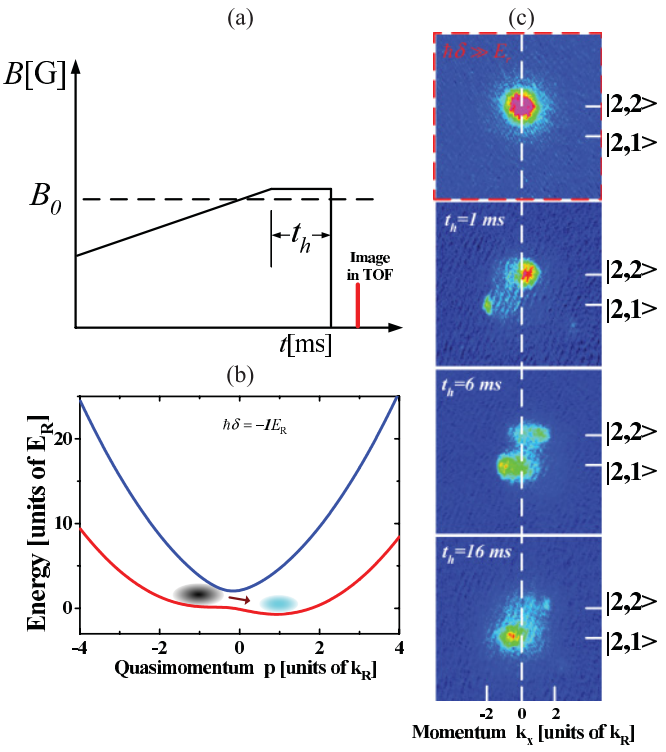

FIG. 3. (Color online) (a) The time sequence for loading the atoms into the low-energy Raman-dressed state. (b) Energy-quasimomentum dispersion for $\hbar\delta = -E_R$ (thick solid curves). The dressed atoms locating at high-energy well of the double wells are unstable and will transit to the low-energy well. (c) Images of the Raman-dressed state for $\hbar\delta = -E_R$ with variable hold times t_h after a 30 ms TOF.

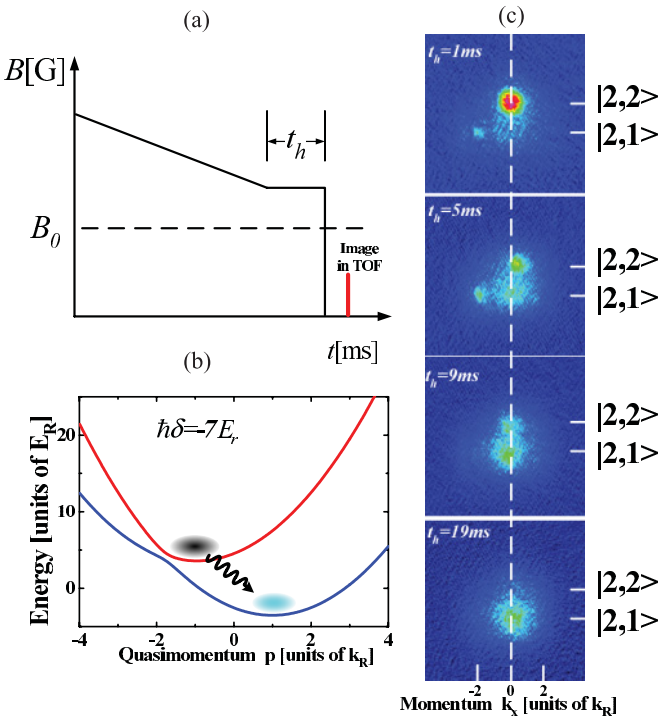

FIG. 4. (Color online) (a) The time sequence for loading the atoms into the high-energy Raman-dressed state. (b) Energy-quasimomentum dispersion for $\hbar\delta = -7E_R$ (thick solid curves) and $\hbar\delta \ll -7E_R$ (thin dashed curves). The atoms start in high-energy Raman-dressed state and ultimately decay into the low-energy Raman-dressed state. (c) Images of the Raman-dressed state for $\hbar\delta = -7E_R$ with variable hold times t_h after a 30 ms TOF.

The homogeneous bias magnetic field is decreased to the value with $\hbar\delta = -7E_R$ and the atoms are loaded to high-energy dressed state adiabatically. The high-energy branch $E_+(p)$ consists of single well in quasimomentum space, thus the dressed atoms locate at $p_{\min} = -0.84k_R$. The dressed atoms in high quasibands are energetically allowed, however, collisional decay will present near Raman resonance except the lowest energy dressed state [10]. The decay for variable hold times ranging from 1 to 19 ms is observed as shown in Fig. 4(c). The dressed atoms in high quasibands decay into the low-energy band accompanying the heating, which is a completely different process compared with that of case 2.

Moreover, the four-photon Raman process with $4\hbar k_R$ momentum is observed, which may be used to generate the light-induced vector gauge potential consisting of the high momentum components. The similar method has been done [30] that the cold atoms were coherently transferred from one dressed state to another one by a multiphoton process, which changed the atom momentum by several photon recoils.

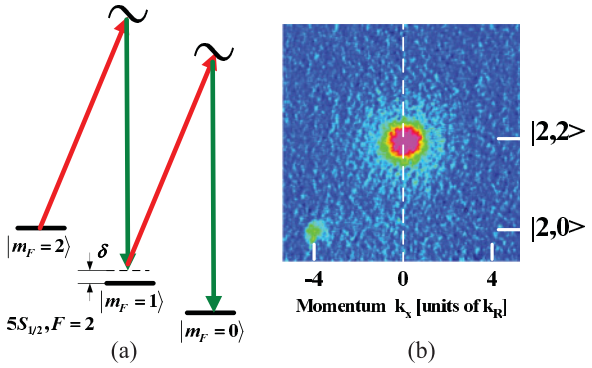

FIG. 5. (Color online) (a) The scheme for generating four-photon Raman process. (b) Images of the four-photon Raman-dressed state after a 30 ms TOF. The two spin and momentum components $|\uparrow, k_x = p_{\min} + 2k_R\rangle$ and $|\tilde{\downarrow}, k_x = p_{\min} - 2k_R\rangle$ are separated along $\hat{y}$.

When the atoms are Raman red detuning with$\delta = -15E_R$ between $|\uparrow\rangle$ and $|\downarrow\rangle$, so the blue detuning between $|\downarrow\rangle$ and $|F = 2, m_F = 0\rangle$ is $+15E_R$, the condition for the four-photon resonant Raman process ($2\nu_R = \omega_Z^{|2,2\rangle \leftrightarrow |2,0\rangle}$) is satisfied as shown in Fig. 5(a). The nonzero two-photon detuning $\delta = \pm 15E_R$ is used to suppress resonant two-photon Raman process. Therefore, the spin state $|F = 2, m_F = 1\rangle$ has negligible contribution in case of the large detuning. We may regard it as the two-level system consisting of $|F = 2, m_F = 2\rangle$ and $|F = 2, m_F = 0\rangle = |\tilde{\downarrow}\rangle$. When ramping the homogeneous bias magnetic field slowly from low field to the four-photon Raman resonance, the atoms are loaded to low-energy dressed state. The two spin and momentum components ($|\uparrow, k_x = p_{\min} + 2k_R\rangle$ and $|\tilde{\downarrow}, k_x = p_{\min} - 2k_R\rangle$) for the dressed state are observed as shown in Fig. 5(b). It will be useful to produce the large size of double wells in quasimomentum space.

In conclusion, we have demonstrated an effective vector gauge potential for ^{87}Rb BEC in the $F = 2$ hyperfine ground state, which was generated by using two crossed 1064-nm optical-dipole-trap lasers to be the Raman beams. The effective vector gauge potential still can be generated (in the atomic long lifetime due to photon scattering in the optical-dipole trap) by the very far detuning (larger than the excited-state fine structure spitting) between the single-photon resonance and the excited state transition, since rubidium has 15 nm the excited-state fine structure spitting [10,31]. The experimental scheme can be applied to produce the synthetic magnetic or electric field by means of a spatial or time dependence of the effective vector potential.

This research is supported by National Basic Research Program of China (Grant No. 2011CB921601), and NSFC (Grant No. 10725416, 60821004).

[1] I. Bloch *et al.*, Rev. Mod. Phys. **80**, 885 (2008).
[2] A. L. Fetter, Rev. Mod. Phys. **81**, 647 (2009).
[3] N. R. Cooper, Adv. Phys. **57**, 539 (2008).
[4] G. Juzeliunas and P. Ohberg, in *Structured Light and its Applications*, edited by D. L. Andrews (Elevier, Amsterdam, 2008).
[5] J. Dalibard *et al.*, e-print arXiv:1008.5378.
[6] J. Ruseckas, G. Juzeliunas, P. Ohberg, and M. Fleischhauer, Phys. Rev. Lett. **95**, 010404 (2005).
[7] S. L. Zhu, H. Fu, C. J. Wu, S. C. Zhang, and L. M. Duan, Phys. Rev. Lett. **97**, 240401 (2006).
[8] X. J. Liu, X. Liu, L. C. Kwek, and C. H. Oh, Phys. Rev. Lett. **98**, 026602 (2007).

[9] K. J. Gunter, M. Cheneau, T. Yefsah, S. P. Rath, and J. Dalibard, Phys. Rev. A **79**, 011604 (2009).
[10] I. B. Spielman, Phys. Rev. A **79**, 063613 (2009).
[11] D. Jaksch and P. Zoller, New J. Phys. **5**, 56 (2003).
[12] A. M. Dudarev, R. B. Diener, I. Carusotto, and Q. Niu, Phys. Rev. Lett. **92**, 153005 (2004).
[13] A. S. Sorensen, E. Demler, and M. D. Lukin, Phys. Rev. Lett. **94**, 086803 (2005).
[14] L. K. Lim, C. M. Smith, and A. Hemmerich, Phys. Rev. Lett. **100**, 130402 (2008).
[15] N. Goldman, A. Kubasiak, A. Bermudez, P. Gaspard, M. Lewenstein, and M. A. Martin-Delgado, Phys. Rev. Lett. **103**, 035301 (2009).
[16] F. Gerbier and J. Dalibard, Phys. Rev. B **81**, 012101 (2010).
[17] N. Goldman, I. Satija, P. Nikolic, A. Bermudez, M. A. Martin-Delgado, M. Lewenstein, and I. B. Spielman, Phys. Rev. Lett. **105**, 255302 (2010).
[18] C. Wang, C. Gao, C. M. Jian, and H. Zhai, Phys. Rev. Lett. **105**, 160403 (2010).
[19] T.-L. Ho and S. Zhang, e-print arXiv:1007.0650.
[20] Z. F. Xu, R. Lu, and L. You, Phys. Rev. A **83**, 053602 (2011).
[21] T. Kawakami *et al*., Phys. Rev. A **84**, 011607(R) (2011).
[22] Y.-J. Lin, R. L. Compton, A. R. Perry, W. D. Phillips, J. V. Porto, and I. B. Spielman, Phys. Rev. Lett. **102**, 130401 (2009).
[23] Y.-J. Lin *et al*., Nature (London) **462**, 628 (2009).
[24] Y-J. Lin *et al*., Nat. Phys. **7**, 531 (2011).
[25] Y.-J. Lin *et al*., Nature (London) **471**, 83 (2011).
[26] D. Wei *et al*., Chin. Phys. Lett. **24**, 679 (2007).
[27] D. Xiong *et al*., Chin. Phys. Lett. **25**, 843 (2008).
[28] D. Xiong *et al*., Opt. Express **18**, 1649 (2010).
[29] D. Xiong *et al*., Chin. Opt. Lett. **8**, 627 (2010).
[30] L. S. Goldner, C. Gerz, R. J. C. Spreeuw, S. L. Rolston, C. I. Westbrook, W. D. Phillips, P. Marte, and P. Zoller, Phys. Rev. Lett. **72**, 997 (1994).
[31] See Supplemental Material at http://link.aps.org/supplemental/10.1103/PhysRevA.84.043609 for the discussion of *Raman coupling strength* and *scattering rate*.